Bioresponsive *pseudo*Glucosinolates (*ps*GSLs) release Isothiocyanates (ITCs) in the Presence of Nitroreductases

Claire C. Jimidar,[b],# Charity S. G. Ganskow,[a],# Mervic D. Kagho,[a],# Aishi Chakrabarti,[a],# Lorenz Wiese,[b] Michael Zollo,[c] Ulrike Beutling,[d] Leona C. Cesar,[a] Julia Morud,[a] Mark Brönstrup,[d] Stephan A. Sieber,[c] Stephan M. Hacker,[e] and Philipp Klahn*[a],[b]

Dedication to Prof. Dr. Stefan Schulz on the occasion of his 66th birthday.

[a] C. S. G. Ganskow, A. Chakrabarti, Dr. Mervic D. Kagho, Leona C. Cesar, Dr. Julia Morud, Prof. Dr. P. Klahn*
Department of Chemistry and Molecular Biology
University of Gothenburg
Natrium, Medicinaregatan 7B, 413 90 Gothenburg, Sweden
E-mail: philipp.klahn@gu.se

[b] C. C. Jimidar, L. Wiese, Prof. Dr. P. Klahn*
Institute of Organic Chemistry
Technische Universität Braunschweig
Hagenring 30, 38106 Braunschweig, Germany

[c] M. Zollo, Prof. Dr. S. A. Sieber
Center for Functional Protein Assemblies
Technische Universität München
Ernst-Otto-Fischer-Straße 8, 85748 Garching, Germany,

[d] U. Beutling, Prof. Dr. M. Brönstrup
Department for Chemical Biology
Helmholtz Center for Infection Research
Inhoffenstraße 7, 38124 Braunschweig, Germany

[e] Dr. S. M. Hacker
Department of Molecular Physiology, Leiden Institute of Chemistry
Leiden University
Einsteinweg 55, 2333 CC Leiden, The Netherlands

# Authors contributed equally.

Supporting information for this article is given via a link at the end of the document.

Abstract: Glucosinolates (GSLs) are secondary metabolites produced as part of an herbivore defence system in plants of the order Brassicales. GSLs release isothiocyanates (ITCs) upon activation by the myrosinase. Beyond their herbivore feeding deterrent properties, these ITCs have multiple interesting bioactivities. However, their release is limited by the presence of myrosinase. Here, we report the concept of *pseudo*glucosinolates (*ps*GSLs) hijacking the natural release mechanism of GSLs for the release of ITCs and adapting it to nitroreductase as the triggering enzymes. We provide proof-of-concept for nitroreductase-responsive *ps*GSLs and demonstrate their potential for peptide labelling, ITC-prodrug approaches and for *in vivo* applications using the nematode of *C. elegans*.

Introduction

Glucosinolates (GSLs) are secondary metabolites produced by plants of the order *Brassicales* such as broccoli, horse radish or white mustard as part of the GSL-myrosinase herbivore defence system.[1] Chemically GSLs are glycosidic thiohydroximate-*O*-sulfonates biogenetically derived from amino acids, which are stored in the tissue of the producing plants separated from the enzyme myrosinase, a thioglucosidase. Upon tissue damage the thioglycosidic bond of the GSLs is cleaved by the myrosinase releasing glucose and a thio-hydroximate-*O*-sulfonate aglycone,[2] which undergoes a subsequent thio-*Lossen* rearrangement forming isothiocyanates (ITCs) as active feeding deterrent agents (Scheme 1A).[3,4] Beyond their feeding deterrent properties, ITCs have raised interest in recent years due to multiple interesting biological activities such as pollinator attraction,[5] antimicrobial activities[6,7] against bee-colony infecting fungi *Nosema ceranae*,[8,9] Methicillin-resistant *Staphylococcus aureus* (MRSA),[10] enterohemorrhagic *Escherichia coli* (EHEC)[11], *Pseudomonas aeruginosa* and related biofilms.[12] In addition, multiple specific bioactivities in mammalian cells have been reported, which might be summarized as neuroprotective, cardioprotective and chemoprotective.[13–18] Most of the biological activities of ITCs seem to be associated with their electrophilic reaction with biological nucleophiles.[11,19,20] GSLs as naturally occurring ITC-releasing molecules have therefore gained interest as intestinal formation of ITCs from GSLs is known to mediate the health beneficiary effects of *Brassicales* enriched dietary.[21–23]

Considering their interesting biological activities, it is not surprising that natural[17,24–28] as well as artificial GSLs have been synthesized including representatives bearing unnatural[17,28,29] or isotopically labeled[29–33] aglycones and

https://doi.org/10.26434/chemrxiv-2024-f8x8z-v2 **ORCID:** https://orcid.org/0000-0003-4713-2345 Content not peer-reviewed by ChemRxiv. **License:** CC BY-NC-ND 4.0

glucose units as well as α-anomeric GSLs.[34,35] Furthermore, artificial GSLs have been designed to serve as myrosinase-responsive tool compounds in chemical biology. In 2018, *Tatibouët* and co-workers, reported the synthesis of mannoside-GSL conjugates, which allowed for myrosinase-triggered specific labelling of lectins[36] with released ITCs or synthesis of glycosylated proteins.[37] In 2019, we reported the synthesis and biochemical evaluation of **GSL-N$_3$** and **GSL-BODIPY** (Scheme 1B), the first examples of an azide bearing and artificial, fluorescent GSL, respectively, forming fluorescent **ITC-BODIPY** in the presence of myrosinase.[38] Independently, Tatibouët and co-workers, reported a similar approach for fluorescent GSLs and demonstrated their ability to serve as labelling probes for proteins.[39] Recently, we have reported also the synthesis of **GSL-DNSA** (Scheme 1B), which was utilized to image uptake through GTR receptors of *Arabidopsis thaliana*.[40] The major limitation for application of these probes in broader chemical biology context is the dependence on myrosinase, a thioglycosidase with limited existence in plants. Beyond that ITCs are hydrolysis sensitive electrophiles showing bad pharmacokinetic properties leaving their interesting biological activities unexploited.[1,41,42]

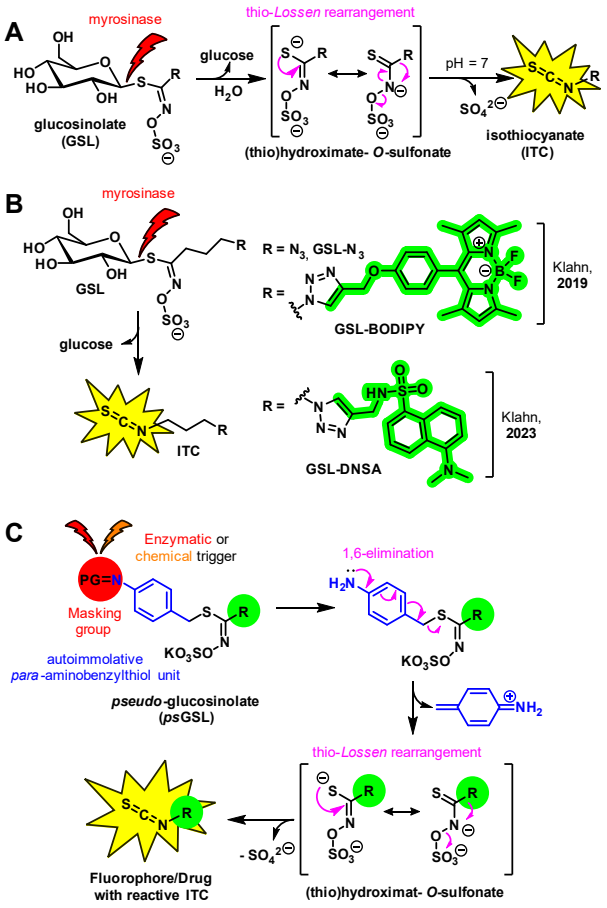

Scheme 1. A: GSL breakdown by myrosinase. **B:** Artificial, fluorescent and azide containing GSLs by *Klahn* and co-workers.[38,40] **C:** Design concept of novel *pseudo*glucosinolates (*ps*GSLs).[48] PG = protective group.

Within our attempts to design bio-responsive molecular entities[43–47] and explore the chemistry of artificial GSLs,[38,40,48] we aimed to translate the natural myrosinase-mediated release mechanism of ITCs from GSLs (Scheme 1A) towards artificial GSLs, which are bioresponsive towards enzymes other than the thioglucosidase myrosinase or even chemical triggers.

Therefore, we envisaged the design of artificial GSLs, in which the thioglycosidic trigger is substituted by a chemically masked *para*-aminobenzylthiol unit (Scheme 1C), which we named *pseudo*glucosinolates (*ps*GSLs).[48] Upon enzymatic or chemical removal of the masking group *ps*GSLs were planned to mimic the natural release mechanism of ITCs from GSLs by undergoing an auto-immolative 1,6-elimination of the free *para*-aminobenzylthiol moiety, leading to the thiohydroximate-*O*-sulfonate as intermediate, followed by the final formation of ITCs through a thio-*Lossen* rearrangement. Thus, *ps*GSLs could serve as prodrugs and tool compounds for the release of ITCs and their response might be adjusted to different non-canonical enzymes and chemical triggers. Within this proof-of-principle study, we aimed to showcase the general *ps*GSL concept within *ps*GSLs releasing ITCs upon reaction with nitroreductases by masking the 1,6-elimination reactivity by a nitro function.

Nitroreductases-responsive prodrugs[49–51] and imaging probes[52,53] based on *para*-nitrobenzyl moieties have been investigated earlier for treatment and imaging of cancer and bacteria, but probes releasing ITCs in the presence of nitroreductases are unknown to date.

Result and Discussion

In order to prove our design concept of *ps*GSLs, we first aimed to synthesize potentially nitroreductase-responsive *ps*GSLs ***ps*GSL(NO$_2$)-N$_3$** and fluorescently labelled ***ps*GSL(NO$_2$)-BODIPY** bearing a nitro-masked *para*-aminobenzylthiol unit as outlined in Scheme 2. For this purpose, commercially available *para*-nitrobenzylalcohol (**1**) was converted into thiol (**4**), which served as nitro-masked *para*-aminobenzylthiol building block. Initial *Appel*-type reaction at -78°C gave access to bromide **2**, which was subsequently substituted in the presence of potassium thioacetate to form the corresponding thioacetate **3**. While basic conditions for the cleavage of the thioacetate led to formation of the respective disulfide, acidic hydrolysis with methanolic HCl under an argon atmosphere provided the desired *para*-nitrobenzyl thiol (**4**) in 89% yield over 3 steps. As building block for the "*pseudo*-aglycone" we synthesized azido oxime **8** starting from the commercially available 2-(4-aminophenyl)ethanol **5**. Formation of the diazonium salt and subsequent substitution with sodium azide gave access to azido alcohol **6**, which was oxidized to the corresponding azido aldehyde **7** using IBX, and final conversion with hydroxylamine led to azido oxime **8** in 39% yield over 3 steps. Both building blocks, **8** and **4**, were coupled adapting the classical approach for the synthesis of GSLs.[24,28,38,54] First azido oxime **8** was converted *in situ* into its respective chloro oxime, and subsequently the substitution of the chloro atom with thiol **4** in the presence of *Hünig's* base facilitated formation of thiohydroximate **9** in 68% yield. Treatment of **9** with pyridine SO_3 complex and subsequent stirring with

https://doi.org/10.26434/chemrxiv-2024-f8x8z-v2 **ORCID:** https://orcid.org/0000-0003-4713-2345 Content not peer-reviewed by ChemRxiv. **License:** CC BY-NC-ND 4.0

aqueous potassium bicarbonate solution gave access to ***ps*GSL(NO$_2$)-N$_3$** in form of its potassium salt in 57% yield. Subsequent copper(I)-catalyzed azide-alkyne cycloaddition click reaction (CuAAC) with *meso*-substituted, alkyne-bearing BODIPY dye **10**[38] led to formation of the fluorescently labelled potential nitroreductase-responsive *ps*GSL, namely ***ps*GSL(NO$_2$)-BODIPY**, in 46% yield.

Unfortunately, although ***ps*GSL(NO$_2$)-N$_3$** was water soluble, the *O*-sulfonate moiety was not sufficient to enable water solubility of ***ps*GSL(NO$_2$)-BODIPY**, a requirement for the biochemical evaluation of the probe in the presence of nitroreductases. As the incorporation of water-soluble groups to the aromatic core of the *para*-aminobenzylthiol unit turned out to be synthetically challenging and flexibility for different fluorescent dyes was desired, we incorporated a PEG$_2$ motif into the core structure as outlined in Scheme 3. To this end, chloride **11** was converted to azide **12** in the presence of sodium azide at 115°C and subsequent *Jones* oxidation gave the ω-azido PEG$_2$ carboxylic acid **13**. *Iso*-butylchloro formate mediated amide coupling with aniline **5** gave alcohol **14** in 63% yield. Oxidation to the aldehyde **15** worked in 86% using IBX. Oxime formation, chlorination, coupling with *para*-nitrophenylthiol **4** and final installation of the *O*-sulfonate proceeded smoothly and gave ***ps*GSL$_{PEG}$(NO$_2$)-N$_3$**. The CuAAC with the dansylamide **18** and BODIPY dye **10**, both bearing a terminal alkyne, provided access to ***ps*GSL$_{PEG}$(NO$_2$)-DNSA** and ***ps*GSL$_{PEG}$(NO$_2$)-BODIPY**, respectively, both showing decent water solubility. All synthesized *ps*GSLs showed decent chemical stability over months stored at -20°C or over weeks stored at 25°C being dissolved in either DMSO, HEPES or TRIS buffer (pH 7.4).

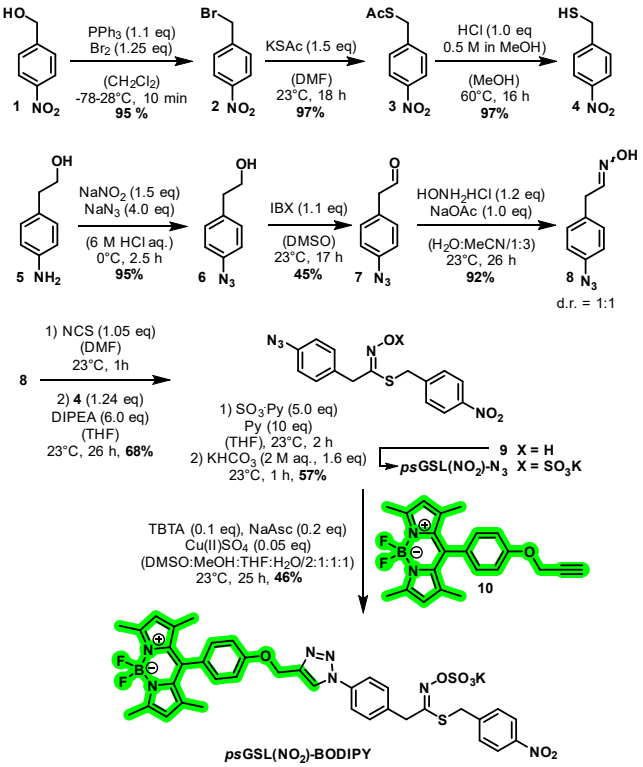

Scheme 2. Synthesis of *para*-nitrobenzylthiol (**4**) and potentially nitroreductase-responsive *ps*GSLs, namely ***ps*GSL(NO$_2$)-N$_3$** and ***ps*GSL(NO$_2$)-BODIPY**.

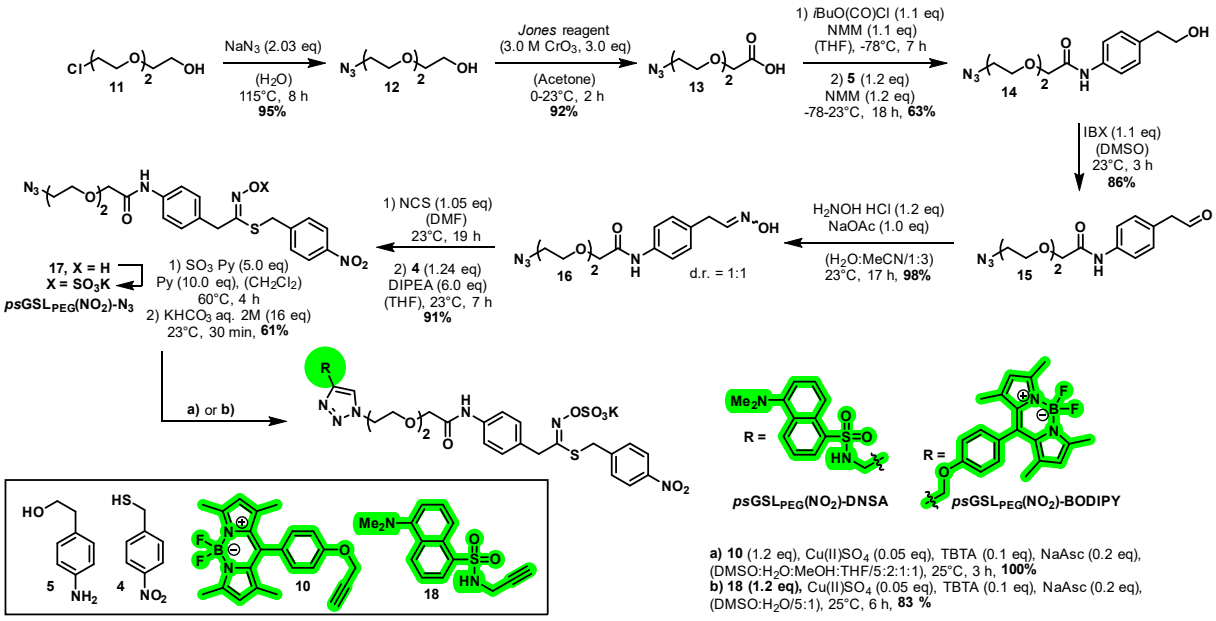

Scheme 3. Synthesis of ***ps*GSL$_{PEG}$(NO$_2$)-N$_3$**, ***ps*GSL$_{PEG}$(NO$_2$)-BODIPY** and ***ps*GSL$_{PEG}$(NO$_2$)-DNSA**.

Next, we tested our hypothesis of ITC release from ***ps*GSL$_{PEG}$(NO$_2$)-N$_3$** in the presence of nitroreductases by LC-MS analysis after incubation of the compounds with the commercially available nitroreductase (NTR) NfsB from *Escherichia coli* and required co-factors NADH and FMN in HEPES buffer (20 mM, pH 7.4) at 37°C.

Coming from the enzymatic investigation of GSLs with the thioglucosidase myrosinase, which shows a relative slow

https://doi.org/10.26434/chemrxiv-2024-f8x8z-v2 **ORCID:** https://orcid.org/0000-0003-4713-2345 Content not peer-reviewed by ChemRxiv. **License:** CC BY-NC-ND 4.0

conversion of their substrates,[38] we first incubated ***ps*GSL$_{PEG}$(NO$_2$)-N$_3$** for 1 h at 37°C. As shown in Figure 1, ***ps*GSL$_{PEG}$(NO$_2$)-N$_3$** (see Figure 1, A: structure, B1: R_t 3.42 min and C1: mass 569 m/z for $[M\text{-}K+2H]^+$) is converted by NfsB and the formation of the corresponding ITC **19** (see Figure 1, A: structure, B2: R_t = 4.10 min, and C3: mass 358 m/z for $[M+Na]^+$ and 336 m/z for $[M+H]^+$) is observed. In addition, we saw the formation of the corresponding hydroxylamine **21** (see Figure 1, A: structure, B2: R_t = 2.63 min, and C2: mass 553 m/z for $[M\text{-}K]^-$).

Furthermore, adding an excess of concentrated aqueous ammonia, both, ITC **19** and hydroxylamine **21** were rapidly converted into the corresponding thiourea **20** within minutes (see Figure 1, A: structure, B3: R_t = 2.33 min, and C4: mass 375 m/z for $[M+Na]^+$, 353 m/z for $[M+H]^+$, 705 m/z for $[2M+H]^+$, and 727 m/z for $[2M+Na]^+$).

Next, we performed several control experiments (See Figure 1, D1-4) for the conversion of ***ps*GSL$_{PEG}$(NO$_2$)-N$_3$** in the absence of the enzyme or cofactors NADH and FMN, with or without subsequent addition of an excess of 30% aqueous ammonia (10 µL ~ 157 µmol ~ 6284-fold excess compared to ***ps*GSL$_{PEG}$(NO$_2$)-N$_3$**).

In none of the control experiments we observed any conversion of ***ps*GSL$_{PEG}$(NO$_2$)-N$_3$**; and in addition the compound was chemically stable under these highly basic conditions. When monitoring the conversion of ***ps*GSL$_{PEG}$(NO$_2$)-N$_3$** in the presence of NfsB and FMN/NADH after 10 min full conversion to the hydroxylamine **21** with only little conversion to the ITC **19** was observed in the LC-MS (See Figure 2, A2).

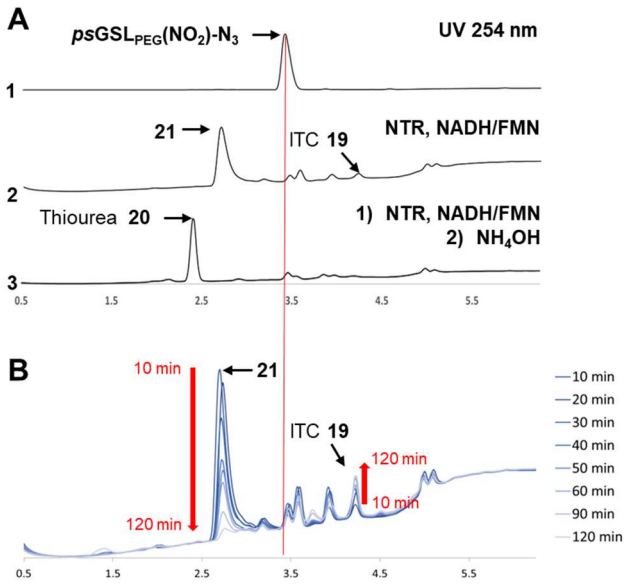

Figure 2. LC-MS analysis after incubation of ***ps*GSL$_{PEG}$(NO$_2$)-N$_3$** with nitroreductase (NTR) NfsB from *E. coli* and subsequent derivatization with NH_4OH solution. **A:** UV chromatogram at 254 nm of (A1) pure ***ps*GSL$_{PEG}$(NO$_2$)-N$_3$** (500 µM) in HEPES buffer (20 mM, pH 7.4), (A2) incubation of ***ps*GSL$_{PEG}$(NO$_2$)-N$_3$** (500 µM) with NfsB (10 µM), NADH (5 mM) and FMN (20 µM) in HEPES buffer (20mM, pH 7.4) after 10 min at 37°C and (A3) A2 and addition of aqueous NH_4OH solution (30 w%, 5 µL) at 23°C. **B:** UV chromatogram at 254 nm of the conversion of ***ps*GSL$_{PEG}$(NO$_2$)-N$_3$** (500 µM) in presence of NfsB (10 µM), NADH (5 mM) and FMN (20 µM) in HEPES buffer (20mM, pH 7.4) over the course of 2 h at 37°C (at t = 10, 20, 30, 40, 50, 60, 90, 120 min).

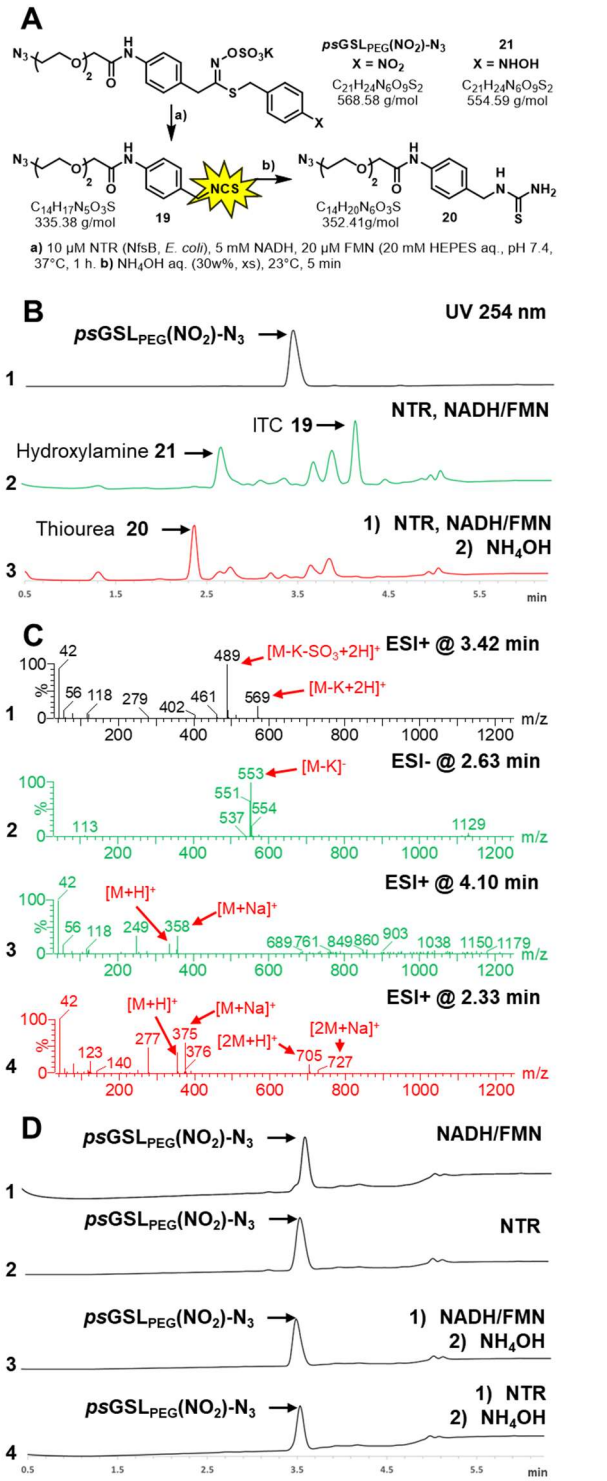

Figure 1. LC-MS analysis after incubation of ***ps*GSL$_{PEG}$(NO$_2$)-N$_3$** with nitroreductase (NTR) NfsB from *E. coli* and subsequent derivatization with NH_4OH solution. **A:** Structures of ***ps*GSL$_{PEG}$(NO$_2$)-N$_3$**, ITC **19**, thiourea **20** and hydroxylamine **21**. **B:** UV chromatogram at 254 nm of (B1) pure ***ps*GSL$_{PEG}$(NO$_2$)-N$_3$** (500 µM) in HEPES buffer (20 mM, pH 7.4), (B2) incubation of ***ps*GSL$_{PEG}$(NO$_2$)-N$_3$** (500 µM) with NfsB (10 µM), NADH (5 mM) and FMN (20 µM) in HEPES buffer (20mM, pH 7.4) after 1 h at 37°C and (B3) A2 and addition of aqueous NH_4OH solution (30 w%, 10 µL). **C:** ESI+ or ESI- mass analysis at (C1) 3.42 min of B1, (C2 and C3) 4.10 min and 2.63 min of B2 and (C4) 2.33 min of B3. **D**: Control experiments following B2 or B3 in absence of NTR (D1 and D3) or the cofactors NADH and FMN (D2 and D3).

https://doi.org/10.26434/chemrxiv-2024-f8x8z-v2 **ORCID:** https://orcid.org/0000-0003-4713-2345 Content not peer-reviewed by ChemRxiv. **License:** CC BY-NC-ND 4.0

Interestingly, both compounds were immediately converted into thiourea **20** when the reaction mixture was treated with an excess of aqueous ammonia (See Figure 2, A3) indicating a corresponding 1,6-elimination from the hydroxylamine **21** and addition of ammonia to the resulting ITC **19**. When the conversion of ***ps*GSL$_{PEG}$(NO$_2$)-N$_3$** in the presence of NfsB and FMN/NADH was monitored over the course of 2 h, **21** was consumed during the reaction under formation of the ITC **19** (Figure 2, B).Considering that hydroxylamines are intrinsic intermediates in the 6-electron reduction of a nitro group to its corresponding amine by nitroreductases (Scheme 4), the observation of **21** as rapidly formed reduction product is reasonable. In addition, the nitroreductase NfsB from *E. coli* belongs to the oxygen insensitive nitroreductases of Type 1 performing two electron reductions[55,56] via a strongly substrate dependent ping-pong-bi-bi mechanism.[57,58] Meaning each 2-electron reduction product has to leave the active centre of the enzyme to allow the binding of a molecule NADH to reduce the prosthetic group FMN[55] again to FMNH$_2$. Afterwards, the release of NAD$^+$ allows binding of the next substrate in the active centre to be further reduced. Strongly depending on the affinity for the substrates, different product distributions are observed for *NsfB*.

Indeed, NfsB is known to contribute to chloramphenicol resistance in Gram-negative bacteria by reduction of chloramphenicol to its corresponding inactive amino-chloramphenicol,[59,60] but likewise induces susceptibility of Gram-negative bacteria towards nitrometronidazol by conversion into its hydroxylamine[60] involved in radical processes damaging the bacterial DNA.

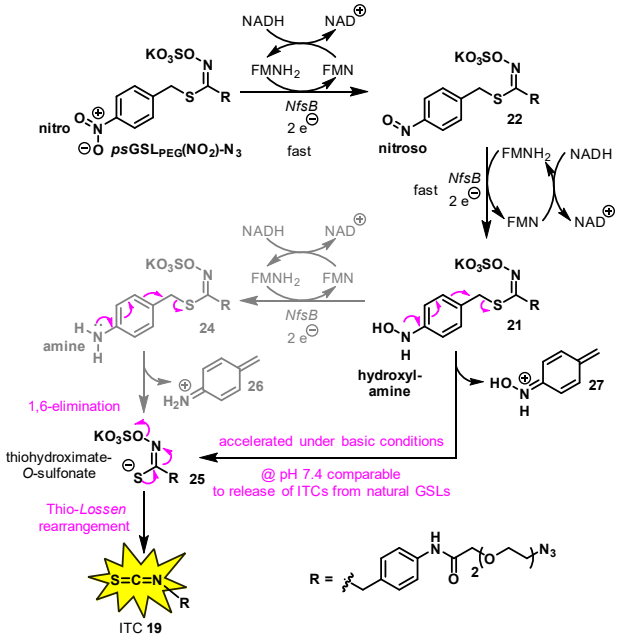

Scheme 4. Proposed reduction of ***ps*GSL$_{PEG}$(NO$_2$)-N$_3$** catalyzed by the Type I oxygen-insensitive nitroreductase (NTR) NfsB from *E. coli* via ping-pong bi-bi mechanism and conversion to ITC **19**.

In our current mechanistic understanding of the overall reaction, the initial reduction of ***ps*GSL$_{PEG}$(NO$_2$)-N$_3$** to the corresponding nitroso compound **22** (only detected in traces, Scheme 4) and subsequently to the hydroxylamine **21** as major reduction product is fast. Whether the corresponding amine **24** (See, Scheme 4) is at all formed during the reaction is not clear. At least we do not detect **24** and it would be a relatively short-living intermediate anyway. However, the envisaged 1,6-elimination forming the thiohydroximate-*O*-sulfonate **25** and subsequent formation of the ITC **19** via thio-*Lossen* rearrangement is observed over 2 h, which is comparable to the slow conversion of natural GSLs into ITCs by myrosinase.[38] In contrast, upon addition of aqueous ammonia under basic conditions the 1,6-elimination and subsequent thio-*Lossen* rearrangement seem to be significantly accelerated.

Similarly, also the fluorophore labelled compounds, ***ps*GSL$_{PEG}$(NO$_2$)-DNSA** and ***ps*GSL$_{PEG}$(NO$_2$)-BODIPY**, showed the release of their corresponding ITCs in the presence of nitroreductase (Figure 3 and 4). When ***ps*GSL$_{PEG}$(NO$_2$)-DNSA** (see Figure 3, A: structure, B1: R_t 3.85 min and C1: mass 857 m/z for [M-K+2H]$^+$ and 777 m/z for [M-K-SO$_3$+2H]$^+$) was incubated with NfsB in the presence of FMN and NADH for 1 h at 37°C, formation of the ITC **26** (see Figure 3, A: structure, B2: R_t 4.65 min and C3: mass 646 m/z for [M+Na]$^+$ and 624 m/z for [M+H]$^+$) alongside with the hydroxylamine **28** (see Figure 3, A: structure, B2: R_t 3.25 min and C2: mass 842 m/z for [M-K]$^-$ and 761 m/z for [M-K-SO$_3$]$^-$) was observed.Again, addition of an excess of concentrated aqueous ammonia, rapidly converted both, ITC **26** and hydroxylamine **28** into the corresponding thiourea **27** within minutes (see Figure 3, A: structure, B3: R_t = 3.32 min, and C4: mass 641 m/z for [M+H]$^+$ and 663 m/z for [M+Na]$^+$).

Next, we wondered if the ITCs formed during the conversion of the *ps*GSLs may label the nitroreductase NfsB through covalent binding.

To prove this, we performed an SDS-PAGE analysis of the reaction mixtures of ***ps*GSL$_{PEG}$(NO$_2$)-DNSA** and ***ps*GSL$_{PEG}$(NO$_2$)-BODIPY** incubated with NfsB, FMN and NADH at 37°C for 2 h (see Figure 4, A). The gel image revealed fluorescent bands at the height of the enzyme when excited at 366 nm for both reactions, indicating a covalent labelling of NfsB (MW: 24727 Da, Uniprot P38489 with a His$_6$-tag).

Additionally in the flow through fluorescent small molecules, presumably corresponding to the fluorescent ITCs **26** and **29** (for structures see Figure 4, C) or their hydrolysis products are visible. Furthermore, we obtained evidence for the covalent adduct by intact protein mass spectrometry. We determined a deconvoluted mass of 24726.9 Da for unmodified NfsB, which matched with the expected mass of 247267.8 Da (Uniprot P38489 with a His$_6$-tag). When ***ps*GSL$_{PEG}$(NO$_2$)-N$_3$** was incubated with NfsB, FMN and NADH at 37°C for 2 h and analyzed by LC/HRMS, we were able to observe the a chromatographic peak for an NfsB variant with 964.9594 m/z with z = 26 corresponding to a that had a deconvoluted protein molecular mass of 25062.9444 Da. The mass shift of +336 Da fits well with the one expected for modification with ITC **19** (+335 Da) within the experimental error of ca. +/- 3 Da reflecting the covalent adduct mass (+336 Da) which matches the expected mass of the utilized nitroreductase NfsB (MW: 24727.8 Da, Uniprot P38489 with a His$_6$-tag) with ITC **19** (compare Figure S1 and

https://doi.org/10.26434/chemrxiv-2024-f8x8z-v2 **ORCID:** https://orcid.org/0000-0003-4713-2345 Content not peer-reviewed by ChemRxiv. **License:** CC BY-NC-ND 4.0

S2 in the Supporting Information). Beyond the labelling of the converting enzyme NfsB, we could demonstrate that bovine serum albumin (BSA, 69.3 kDa, Uniprot P02769) added to the reaction mixture was also labelled efficiently with ***ps*GSL$_{PEG}$(NO$_2$)-BODIPY** in the presence of NfsB as show in Figure 4 B.

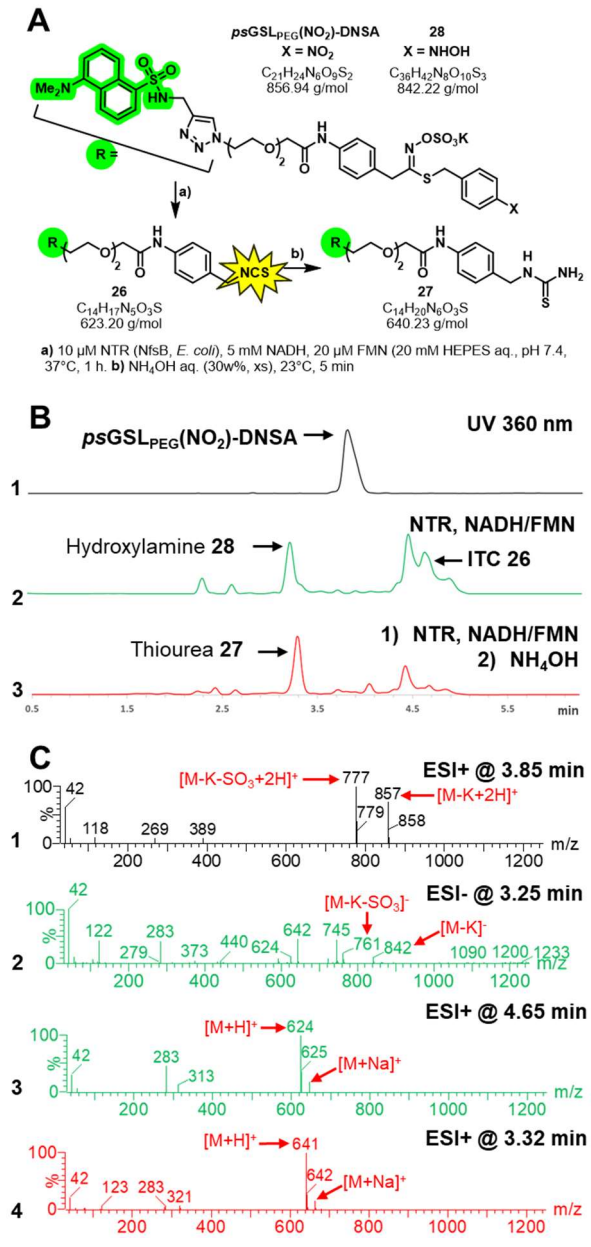

Figure 3. LC-MS analysis after incubation of ***ps*GSL$_{PEG}$(NO$_2$)-DNSA** with nitroreductase (NTR) NfsB from *E. coli* and subsequent derivatization with NH$_4$OH solution. **A:** Structures of ***ps*GSL$_{PEG}$(NO$_2$)-DNSA**, ITC **26**, thiourea **27** and hydroxylamine **28**. **B:** UV chromatogram at 254 nm of (B1) pure ***ps*GSL$_{PEG}$(NO$_2$)-DNSA** (500 µM) in HEPES buffer (20 mM, pH 7.4), (B2) incubation of ***ps*GSL$_{PEG}$(NO$_2$)-DNSA** (500 µM) with NfsB (10 µM), NADH (5 mM) and FMN (20 µM) in HEPES buffer (20mM, pH 7.4) after 1 h at 37°C and (B3) A2 and addition of aqueous NH$_4$OH solution (30 w%, 10 µL) at 23°C. **C:** ESI+ or ESI- mass analysis at (C1) 3.85 min of B1, (C2 and C3) 3.25 min and 4.65 min of B2 and (C4) 3.32 min of B3.

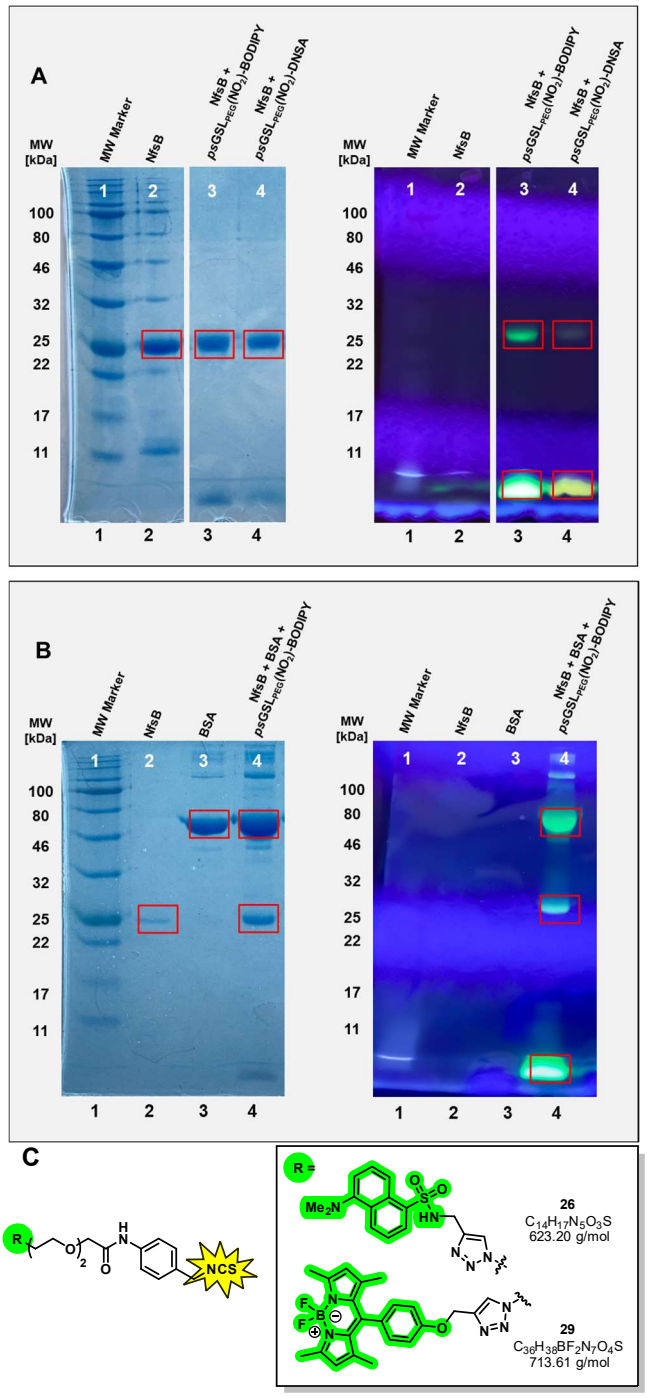

Figure 4. A: SDS-PAGE gel analysis of the conversion of ***ps*GSL$_{PEG}$(NO$_2$)-BODIPY** and ***ps*GSL$_{PEG}$(NO$_2$)-DNSA** in the presence of nitroreductase (NTR) NfsB from *E. coli*, left: visible light/Coomassie blue™ stain, right: UV light (366 nm), (1) molecular weight marker (3 µL, 2 mg/mL), (2) nitroreductase NfsB (10 µL, 2 mg/mL), (3) 10 µL of ***ps*GSL$_{PEG}$(NO$_2$)-BODIPY** (500 µM) with NfsB (10 µM), NADH (5 mM) and FMN (20 µM) in HEPES buffer (20mM, pH 7.4) after 2 h at 37°C, (4) 10 µL of ***ps*GSL$_{PEG}$(NO$_2$)-DNSA** (500 µM) with NfsB (10 µM), NADH (5 mM) and FMN (20 µM) in HEPES buffer (20mM, pH 7.4) after 2 h at 37°C. **B:** SDS-PAGE gel analysis of the labelling of bovine serum albumin (BSA) with ***ps*GSL$_{PEG}$(NO$_2$)-BODIPY** in the presence of nitroreductase (NTR) NfsB from *E. coli*, left: visible light/Coomassie blue™ stain, right: UV light (366 nm), (1) molecular weight marker (3 µL, 2 mg/mL), (2) nitroreductase NfsB (10 µL, 0.5 mg/mL), (3) BSA (10 µL, 2 mg/mL), (4) 10 µL of ***ps*GSL$_{PEG}$(NO$_2$)-BODIPY** (500 µM) with NfsB (10 µM), NADH (5 mM) and FMN (20 µM) in HEPES buffer (20mM, pH 7.4) and BSA (2 mg/mL) after 2 h at 37°C. **C:** Structures of ITCs **26** and **29.**

https://doi.org/10.26434/chemrxiv-2024-f8x8z-v2 **ORCID:** https://orcid.org/0000-0003-4713-2345 Content not peer-reviewed by ChemRxiv. **License:** CC BY-NC-ND 4.0

ITCs have been demonstrated to covalently bind peptides via irreversible formation of thioureas upon reacting with lysine residues or via reversible formation of dithiocarbamates upon reacting with cysteine residues.[61–63] While the pH optimum for the thiourea formation has been shown to be between pH 9-11, dithiocarbamates form predominately at pH 6-8.[62] Although dithiocarbamates might be the initially formed adducts, they might function as resting intermediate, reforming the ITC and finally leading to lysine thiourea adducts as stable modifications.[61]

To further elucidate how ITCs released from *ps*GSLs covalently bind to a given proteome, we next performed a chemoproteomics experiment in the proteome of Staphylococcus aureus SH1000 utilizing our isotopically labelled desthiobiotin-activity-based protein profiling technology (isoDTB-ABPP),[64,65] which is based on the isotopic tandem orthogonal proteolysis-ABPP (isoTOP-ABPP)[66,67] platform. Specifically, we utilized an MSFragger[64,65] based workflow that we recently established to monitor electrophile reactivity and selectivity in a completely unbiased fashion.[65]

To be compatible with the azide-containing isoDTB tags, the nitroreductase-responsive probe ***ps*GSL(NO2)-alkyne** was synthesized from hex-5-yn-1-ol (**30**) as outlined in Scheme 5. Similar as before, the nitroreductase-responsive probe ***ps*GSL(NO_2)**-alkyne was synthesized from hex-5-yn-1-ol (**30**) as outlined in Scheme 5. Oxidation of **30** with IBX and subsequent conversion with hydroxylamine gave oxime **31** as 1:1-mixture of diastereoisomers in 67% yield.

Formation of the chloro oxime and subsequent coupling with para-nitrobenzylthiol (**4**) gave the thiohydroximate **32**, which was treated with pyridine SO_3 complex and potassium hydrogen carbonate solution to obtain ***ps*GSL(NO_2)-alkyne**. With ***ps*GSL(NO_2)-alkyne** in hand, two identical samples of freshly prepared lysate of *S. aureus* SH1000 were incubated with the probe in presence of nitroreductase NfsB from *E. coli*, FMN and NADH for 1 h at 37°C (see Figure 5A) to form protein adducts.

In one sample the heavy isoDTB-tag was attached to the terminal alkyne via CuAAC and in the other one the corresponding light isoDTB-tag. Afterwards the samples were combined and a pull-down of isoDTB-labelled proteins utilizing streptavidin-agarose beads was performed. The enriched protein fractions were digested, subjected to a streamlined mass sample preparation and the modified peptides were analyzed by LC-MS/MS.

Surprisingly, the almost exclusively observed proteome modification was found to be an amidine instead of the expected thiourea obtained in the other experiments performed (Figure 5B).

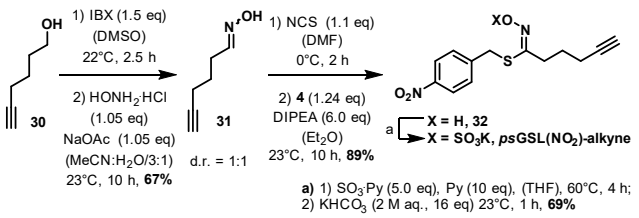

Scheme 5. Synthesis of ***ps*GSL(NO_2)-alkyne**.

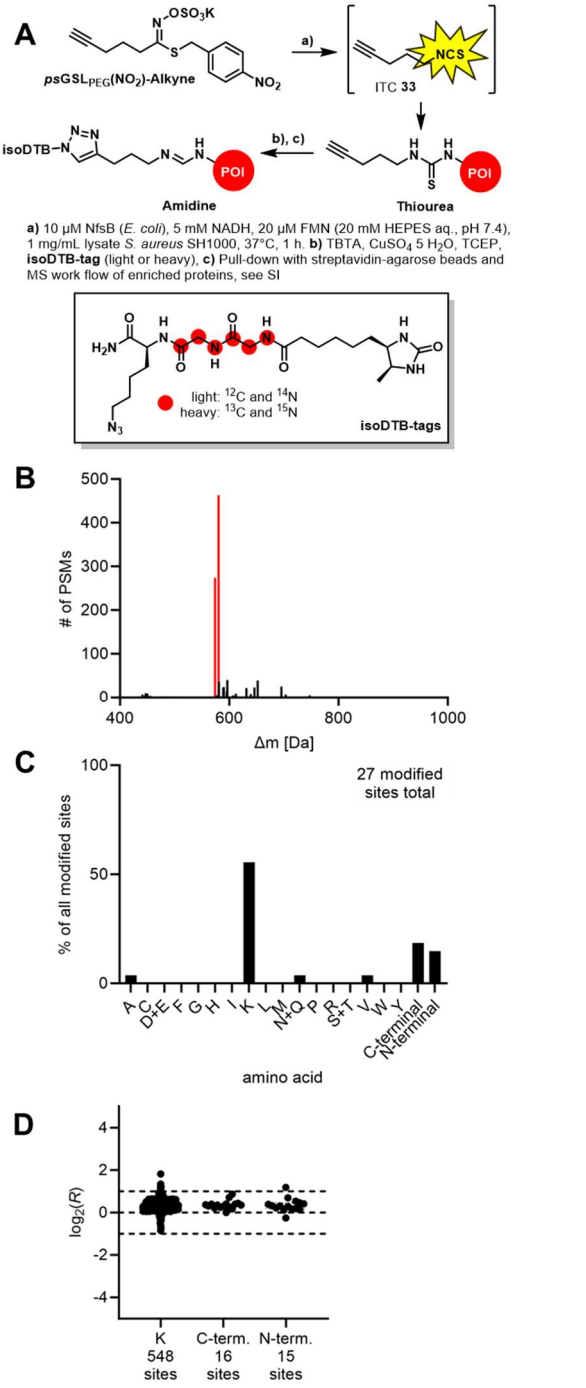

Figure 5. Labelling of *S. aureus* SH1000 proteome (at 1 mg/mL) with 100 µM of ***ps*GSL(NO_2)-alkyne** using the isoDTB-ABPP workflow[64]: **A:** Structures of ***ps*GSL(NO_2)-alkyne**, ITC **33** and the heavy and light **isoDTB-tags**; general structures of thioureas and isoDTB-tag-clicked amidines (POI = protein of interest). **B:** Masses of modification determined through analysis with an Open Search in MSFragger[68,69] **C:** Amino acid selectivity determined through an Offset Search that localizes the modification to the modified amino acid(s) In this way, selectivity is assessed across all proteinogenic amino acids. The bar represents the fraction of all modified sites that is modified at the indicated amino acid. **D:** Quantification of the modification at the main amino acid residues identified in the offset search at the selected masses was performed using a Closed Search and the IonQuant[70] feature. The heavy and light samples were mixed at a ratio of 1:1. The dashed lines indicate the expected values of log2(*R*) = 0 and the preferred window of quantification (−1 < log2(*R*) < 1). All data is based on technical duplicates**.** For a representative MS/MS spectrum with the relative b and y ions, see Figure S3 in the Supporting Information.

https://doi.org/10.26434/chemrxiv-2024-f8x8z-v2 **ORCID:** https://orcid.org/0000-0003-4713-2345 Content not peer-reviewed by ChemRxiv. **License:** CC BY-NC-ND 4.0

Currently, we believe that a substrate-dependent, acid-catalyzed desulfurization is occurring in presence of TFA during the sample preparation of the isoDTB-ABPP workflow or during ionization in the LCMS. Oxidative formation of amidines from thioureas is known in the presence of strong oxidants such as hydrogen peroxide under acidic conditions already at 25°C.[71] Attempts to facilitate amidine formation under similar conditions led to formation of only traces of corresponding amidines in presence of formic acid or TFA at 23°C. (See Figure S4 in the Supporting Information). We ruled out a direct reaction of ***ps*GSL(NO$_2$)-alkyne** with lysine residues, as no reaction of ***ps*GSL(NO$_2$)-alkyne** with BSA or lysine is observed in the absence of NfsB and as shown in Figure 1D *ps*GSLs is stable in the presence of high concentration of nitrogen nucleophiles even at pH 14. The exact mechanism and nature of this desulfurization is still under investigation. However, according to the isoDTB-ABPP workflow this is the main modification that is detected by chemoproteomic analysis (for a representative MS/MS spectrum with the relative b and y ions, see Figure S3 in the Supporting Information).

We next used the mass of modification of amidine formation as input for an offset search to study the amino acid selectivity (Figure 5C).[65] The modification was mainly localized to amino groups in the detected proteins (lysines and protein *N*-termini) as expected with some surprising reactivity also at protein *C*-termini. Overall, the modification does not seem to be very stable under the detection conditions as seen by the low number of localized sites after the application of the very stringent filters of the offset search (27 sites unambiguously localized). This indicates that the modification is easily lost upon fragmentation in the mass spectrometer. As discussed above, modification of cysteines with ITCs is expected to be reversible, explaining why cysteine modification cannot be detected in this experiment. Overall, the amidine modification of the proteome mainly localized to lysines and the protein termini.

In the final stage of the isoDTB-ABPP analysis, we quantified the residues that are modified with the amidine modification. It is striking, that under the less stringent localization filters used for quantification, we mainly identify lysine modification indicating that stability of the modification at lysines is the main limitation to high quality localization and that the probe mainly leads to lysine-modified peptides. Of the 548 modified lysine sites, the vast majority was quantified with a small spread around the expected $\log_2(R)$ of 0 indicating reliable quantification of these modified peptides. Among the 548 modified lysines were 265 that were identified in 89 different essential proteins. These include lysines in important functional sites of the proteins such as those forming Schiff Bases during catalysis (K82 of pyridoxal 5'-phosphate synthase pdxS and K151 of deoxyribose-phosphate aldolase deoC), other residues at active sites (K596 of glutamine-fructose-6-phosphate aminotransferase glmS and K217 of ribitol-5-phosphate cytidylyltransferase 1 tarI), residues at nucleotide binding sites (K71 at the ATP binding site of formate-tetrahydrofolate ligase fhs, K23 at the GTP binding site of elongation factor G fusA and K46 of the ATP binding site of succinate-CoA ligase sucC) and, strikingly, at DNA binding sites of transcriptional regulators (K52 and K56 of HTH-type transcriptional regulator SarR and K57 and K74 of HTH-type transcriptional regulator MgrA). While the performed isoDTB-ABPP experiment does not inform on the stoichiometry of engagement at these residues, it is a good indication that ITCs can exert an effect in bacteria through engagement of a variety of functional lysines in proteins.

Finally, we wondered if the conversion of *ps*GSLs in presence of nitroreductase could also be achieved in living organisms, thus allowing for *in vivo* labelling of amines and lysine residues. Therefore, we aimed to release the BODIPY-labelled ITC **29** (compare Figure 4C) in the presence of NfsB in living *Caenorhabditis elegans* as an easy-to-handle model organism expecting to label free amines through covalent binding present in intestinal membranes. To investigate this, day 1 adult *C. elegans* worms were pre-incubated with ***ps*GSL$_{PEG}$(NO$_2$)-BODIPY** for 1 h at 23°C, before NfsB, FMN and NADH was added for a 2 h incubation at 23°C, followed by an immediate washing step with M9 buffer for 2 h (see Figure 6C).

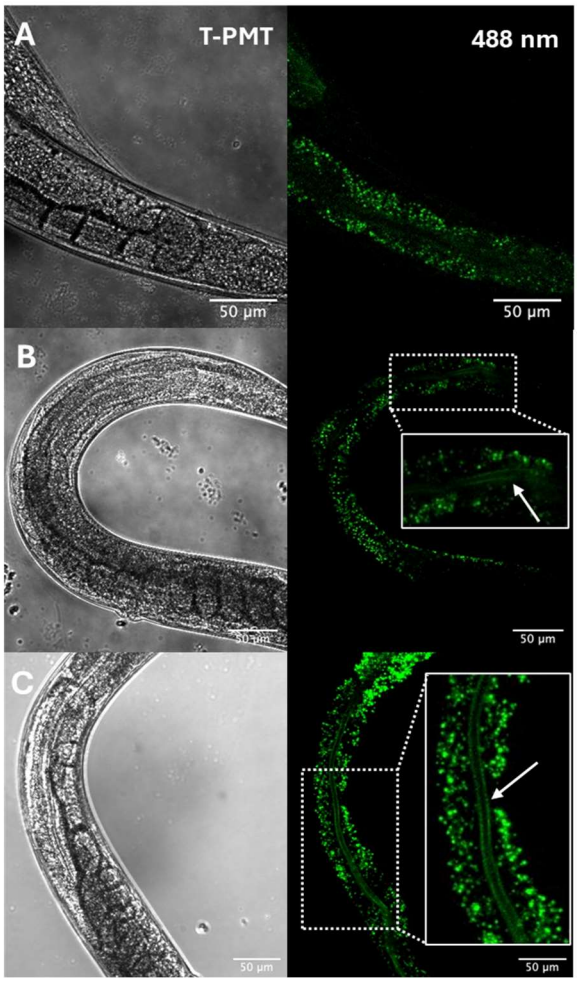

Figure 6. Fluorescence microscopy imaging of *C. elegans* 24 h after an initial pre-incubation step with ***ps*GSL$_{PEG}$(NO$_2$)-BODIPY** for 1 h. **A**: pre-incubation with ***ps*GSL$_{PEG}$(NO$_2$)-BODIPY** at 23°C (but no NfsB or co-factors). **B:** 1***ps*GSL$_{PEG}$(NO$_2$)-BODIPY** at 23°C and 2 h incubation with co-factors NADH and FMN at 23°C (but no NfsB). **C:** 1 h pre-incubation with ***ps*GSL$_{PEG}$(NO$_2$)-BODIPY** at 23°C and 2 h incubation with external nitro-reductase (NfsB) from *E. coli* and co-factors NADH and FMN at 23°C. All conditions included washing out of excessive unconsumed and unbound ***ps*GSL$_{PEG}$(NO$_2$)-BODIPY** for 2 h with M9 buffer as well as 24 h incubation on NGM plates in presence of OP50 *E. coli.*

https://doi.org/10.26434/chemrxiv-2024-f8x8z-v2 **ORCID:** https://orcid.org/0000-0003-4713-2345 Content not peer-reviewed by ChemRxiv. **License:** CC BY-NC-ND 4.0

As controls, the worms were incubated with ***ps*GSL$_{PEG}$(NO$_2$)-BODIPY** alone (see Figure 6A) and ***ps*GSL$_{PEG}$(NO$_2$)-BODIPY** and the co-factors FMN and NADH but without external nitro-reductase (NfsB) from *E. coli* (see Figure 6B). After the excess of ***ps*GSL$_{PEG}$(NO$_2$)-BODIPY**, NfsB, FMN and NADH were washed out, confocal fluorescence microscopy imaging of the worms was carried out at 488 nm 24 h after initial incubation with ***ps*GSL$_{PEG}$(NO$_2$)-BODIPY**. To our delight, pre-incubation with ***ps*GSL$_{PEG}$(NO$_2$)-BODIPY** followed by subsequent incubation with NfsB and co-factors led to strong fluorescent labelling of the membrane of the intestinal lumen (see Figure 6A, Green dots are naturally occurring gut granules in the intestine of the worms). In contrast, when incubation was performed with only ***ps*GSL$_{PEG}$(NO$_2$)-BODIPY,** without NfsB and the co-factors NADH and FMN, no specific signal after 24 h was detected, except for a diffuse signal in the intestinal lumen arising from potentially unbound compound (see Figure 6A). When we performed the incubation with the cofactors only, not adding external NfsB, a weak and diffuse signal was observed in only a few of the worms in the very posterior part of the intestinal lumen (see Figure 6B). This finding is reasonable as the worms feed on *E. coli*, thus, endogenous NTR from intestinal *E. coli* lysate might lead to a low degree conversion of the probe.

Therefore, the specificity in NfsB mediated ITC formation leading to covalent labelling is clearly shown in these experiments and serves as a first *in vivo* proof-of-concept, which can be widely expanded into further applications. Furthermore, it is worth mentioning that all worms survived the treatment with ***ps*GSL$_{PEG}$(NO$_2$)-BODIPY** and were not particularly affected by the ITC **29**. Additionally, the worms displayed a normal broad size with no obvious developmental effects in the new generation.

Conclusion

Here, we have introduced the concept of *pseudo*glucosinolates (*ps*GSLs) that can be activated into isothiocyanantes (ITCs) with non-canonical enzymes. We have demonstrated the release of ITCs from ***ps*GSL$_{PEG}$(NO$_2$)-N$_3$**, ***ps*GSL$_{PEG}$(NO$_2$)-BODIPY**, ***ps*GSL$_{PEG}$(NO$_2$)-DNSA** and ***ps*GSL(NO$_2$)-alkyne** in the presence of nitroreductase NfsB from *E. coli*. The released ITCs were demonstrated to be effective in labelling of BSA and show a predominantly lysine-selective modification of proteins in the entire proteome including many functional sites of essential proteins. Additionally, we performed NfsB-mediated ITC formation and subsequent covalent BODPIY-labeling of the membrane in the intestinal lumen of *C. elegans* demonstrating conversion, functionality and tolerability of the probes *in vivo*.

In contrast to natural GSLs, *ps*GSLs represent a complementary prodrug approach for bio-responsive release of ITCs, which hold potential to be adjusted in their bio-responsiveness towards multiple enzymes and chemical microenvironments. The concept of *ps*GSLs might find application in chemical biology for enzyme-dependent labelling of biomolecules and prodrug approaches to exploit the broad variety of interesting biological activities of potentially hydrolysis sensitive ITCs.[20]

Currently, the protection of the *para*-aminobenzylthiol unit with different peptidase-, oxidoreductase- and hydrolases-responsive masking groups is under investigation to expand the concept of *ps*GSLs towards a platform technology for bio-responsive protein labelling and ITC-based covalent inhibitors of proteins.

Supporting Information

The authors have cited additional references within the Supporting Information.[64,65,68–70,72–84]

Acknowledgements

Parts of this work have been carried out within the framework of the SMART BIOTECS alliance between the Technische Universität Braunschweig and the Leibniz Universität Hannover. This initiative is supported by the Ministry of Science and Culture (MWK) of Lower Saxony, Germany. Financial support by the Max-Buchner Foundation (Max-Buchner Fellowship for PK), Deutsche Forschungsgemeinschaft (DFG, grant KL3012/2-1 (PK) and grant KL3012/4-1 (PK)), the Fonds der Chemischen Industrie (FCI, PK, SMH), Vetenskapsrådet (VR Starting Grant 2022-03951, JM), Swedish Foundation for Strategic Research (SSF, FFL21-0166, JM), the Studienstiftung des Deutschen Volkes (MZ), the Marianne-Plehn-Program (MZ) as well as the starting funds of PK at University of Gothenburg is gratefully acknowledged. The authors thank the Swedish NMR Center (SNC, GU), The Centre of Cellular Imaging (CCI, GU), the Swedish National Microscopy Infrastructure, the Proteomics Core Facility (PFC, GU), the mass spectrometry and NMR spectroscopy units of the Institute of Organic Chemistry (TUBS), and Dr. Daniel Tietze (GU) for analytical support. The content of this work is solely the responsibility of the authors and does not necessarily represent the official views of the funding agencies.

Author contributions

Contribution are given with CRediT definition according to Brand *et al.*[85]

Conceptualization: PK; Methodology: CCJ, CSGG, MDK, AC, LW, MZ, LCC, JML and UB; Software: - ; Validation: CSGG, MZ and CCJ; Formal analysis: MZ; Investigation: CCJ, CSGG, MDK, AC, LW, MZ, LCC, JM and UB; Resources: PK, MB, SAS, SMH and JM; Data curation: PK; Writing—original draft: CSGG, CCJ, AC, MDK, MZ, SMH and PK; Writing—review & editing: all authors; Visualization: PK, AC, CSGG, MDK, MZ, JM and SMH; Supervision: PK, MB, SAS, JM and SMH; Project administration: PK; Funding acquisition: PK, MB, SAS, JM and SMH.

Keywords: *pseudo*glucosinolates • artificial glucosinolates • isothiocyanates • bioresponsive protein labelling • prodrug

https://doi.org/10.26434/chemrxiv-2024-f8x8z-v2 **ORCID:** https://orcid.org/0000-0003-4713-2345 Content not peer-reviewed by ChemRxiv. **License:** CC BY-NC-ND 4.0

[1] F. S. Hanschen, E. Lamy, M. Schreiner, S. Rohn, *Angew. Chem. Int. Ed.* **2014**, *53*, 11430–11450.

[2] A. M. Bones, J. T. Rossiter, *Phytochemistry* **2006**, *67*, 1053–1067.

[3] I. Winde, U. Wittstock, *Phytochemistry* **2011**, *72*, 1566–1575.

[4] J.-M. Mérillon, K. G. Ramawat, Eds. , *Glucosinolates*, Cham, **2017**.

[5] S. D. Johnson, M. E. Griffiths, C. I. Peter, M. J. Lawes, *Am. J. Bot.* **2009**, *96*, 2080–2086.

[6] L. Romeo, R. Iori, P. Rollin, P. Bramanti, E. Mazzon, J. W. Fahey, A. T. Zalcmann, P. Talalay, *Molecules* **2018**, *23*, 624.

[7] M. G. Kim, H. S. Lee, *J. Food Sci.* **2009**, *74*, 467–471.

[8] L. Ugolini, G. Cilia, E. Pagnotta, L. Malaguti, V. Capano, I. Guerra, L. Zavatta, S. Albertazzi, R. Matteo, L. Lazzeri, L. Righetti, A. Nanetti, *Biomolecules* **2021**, *11*, 1657.

[9] A. Nanetti, L. Ugolini, G. Cilia, E. Pagnotta, L. Malaguti, I. Cardaio, R. Matteo, L. Lazzeri, *Microorganisms* **2021**, *9*, 949.

[10] C. Dias, A. Aires, M. Saavedra, *Int. J. Mol. Sci.* **2014**, *15*, 19552–19561.

[11] D. Nowicki, O. Rodzik, A. Herman-Antosiewicz, A. Szalewska-Pałasz, *Sci. Rep.* **2016**, *6*, 22263.

[12] S. J. Kaiser, N. T. Mutters, B. Blessing, F. Günther, *Fitoterapia* **2017**, *119*, 57–63.

[13] C. Melim, M. R. Lauro, I. M. Pires, P. J. Oliveira, C. Cabral, *Pharmaceutics* **2022**, *14*, 190.

[14] J. Melrose, *Biomedicines* **2019**, *7*, 62.

[15] E. L. Connolly, M. Sim, N. Travica, W. Marx, G. Beasy, G. S. Lynch, C. P. Bondonno, J. R. Lewis, J. M. Hodgson, L. C. Blekkenhorst, *Front. Pharmacol.* **2021**, *12*, Article 767975.

[16] P. Soundararajan, J. Kim, *Molecules* **2018**, *23*, 2983.

[17] Q. V. Vo, C. Trenerry, S. Rochfort, J. Wadeson, C. Leyton, A. B. Hughes, *Bioorg. Med. Chem.* **2013**, *21*, 5945–5954.

[18] N. Orouji, S. K. Asl, Z. Taghipour, S. Habtemariam, S. M. Nabavi, R. Rahimi, *Med. Oncol.* **2023**, *40*, 344.

[19] Ł. Janczewski, *Molecules* **2022**, *27*, 1750.

[20] X. Tian, J. Gao, M. Liu, Y. Lei, F. Wang, J. Chen, P. Chu, J. Gao, F. Long, M. Liang, X. Long, H. Chu, C. Liu, X. Li, Q. Sun, G. Li, Y. Yang, *J. Med. Chem.* **2020**, *63*, 3881–3895.

[21] A. Narbad, J. T. Rossiter, *Mol. Nutr. Food Res.* **2018**, *62*, 1–10.

[22] C. S. Liou, S. J. Sirk, C. A. C. Diaz, A. P. Klein, C. R. Fischer, S. K. Higginbottom, A. Erez, M. S. Donia, J. L. Sonnenburg, E. S. Sattely, *Cell* **2020**, *180*, 717-728.e19.

[23] V. Luang-In, A. A. Albaser, C. Nueno-Palop, M. H. Bennett, A. Narbad, J. T. Rossiter, *Curr. Microbiol.* **2016**, *73*, 442–451.

[24] D. Cerniauskaite, J. Rousseau, A. Sackus, P. Rollin, A. Tatibouët, *Eur. J. Org. Chem.* **2011**, 2293–2300.

[25] W. Abramski, M. Chmielewski, *J. Carbohydr. Chem.* **2006**, *15*, 109–113.

[26] M. S. C. Pedras, Q. H. To, G. Schatte, *Chem. Commun.* **2016**, *52*, 2505–2508.

[27] M. Mavratzotis, S. Cassel, S. Montaut, P. Rollin, *Molecules* **2018**, *23*, 1–15.

[28] Y. W. Lim, M. J. H. Ong, R. J. Hewitt, *Synthesis* **2018**, *50*, 1640–1650.

[29] J. J. Morrison, N. P. Botting, A. A. B. Robertson, *J Label Compd Radiopharm* **2007**, *50*, 260–263.

[30] N. P. Botting, A. A. B. Robertson, J. J. Morrison, *J. Label. Compd. Radiopharm.* **2007**, *50*, 260–263.

[31] J. T. Rossiter, J. A. Pickett, M. H. Bennett, A. M. Bones, G. Powell, J. Cobb, *Phytochemistry* **2007**, *68*, 1384–1390.

[32] M. S. C. Pedras, Q. H. To, *J. Label. Compd. Radiopharm.* **2018**, *61*, 94–106.

[33] Q. Zhang, T. Lebl, A. Kulczynska, N. P. Botting, *Tetrahedron* **2009**, *65*, 4871–4876.

[34] M. Blanc-Muesser, H. Driguez, B. Joseph, M. C. Viaud, P. Rollin, *Tetrahedron Lett.* **1990**, 3867–3868.

[35] Q. V. Vo, S. Rochfort, P. C. Nam, T. L. Nguyen, T. T. Nguyen, A. Mechler, *Carbohydr. Res.* **2018**, *455*, 45–53.

[36] G. Cutolo, F. Reise, M. Schuler, R. Nehmé, G. Despras, J. Brekalo, P. Morin, P.-Y. Renard, T. K. Lindhorst, A. Tatibouët, *Org. Biomol. Chem.* **2018**, *16*, 4900–4913.

[37] G. Cutolo, B. Didak, J. Tomas, B. Roubinet, P. Lafite, R. Nehmé, M. Schuler, L. Landemarre, A. Tatibouët, *Carbohydr. Res.* **2022**, *516*, 108562.

[38] C. P. Glindemann, A. Backenköhler, M. Strieker, U. Wittstock, P. Klahn, *ChemBioChem* **2019**, *19*, 1668–1694.

[39] C. Sabot, J. W. Fredy, G. Cutolo, B. Poret, R. Nehmé, M. Hubert-Roux, P. Gandolfo, H. Castel, M. Schuler, A. Tatibouët, P.-Y. Renard, *Bioconjug. Chem.* **2019**, *30*, 1385–1394.

[40] C. Kanstrup, C. C. Jimidar, J. Tomas, G. Cutolo, C. Crocoll, M. Schuler, P. Klahn, A. Tatibouët, H. H. Nour-Eldin, *Int. J. Mol. Sci.* **2023**, *24*, 920.

[41] J. Zhang, X. Li, P. Ge, B. Zhang, L. Wen, C. Gu, X. Zhou, *Sep. Purif. Rev.* **2022**, *51*, 330–339.

[42] G. Tian, P. Tang, R. Xie, L. Cheng, Q. Yuan, J. Hu, *Food Chem.* **2016**, *199*, 301–306.

[43] C. C. Jimidar, J. Grunenberg, B. Karge, H. L. S. Fuchs, M. Brönstrup, P. Klahn, *Chem. – A Eur. J.* **2022**, *28*, e202103525.

[44] O. A. Okoh, P. Klahn, *ChemBioChem* **2018**, *19*, 1668–1694.

[45] P. Klahn, V. Fetz, A. Ritter, W. Collisi, B. Hinkelmann, T. Arnold, W. Tegge, K. Rox, S. Hüttel, K. I. K. I. Mohr, J. Wink, M. Stadler, J. Wissing, L. Jänsch, M. Brönstrup, *Chem. Sci.* **2019**, *10*, 5187–5425.

[46] Y. Bourgat, C. Mikolai, M. Stiesch, P. Klahn, H. Menzel, *Antibiotics* **2021**, *10*, 653.

[47] R. Zscherp, J. Coetzee, J. Vornweg, J. Grunenberg, J. Herrmann, R. Müller, P. Klahn, *Chem. Sci.* **2021**, *12*, 10179–10190.

[48] C. C. Jimidar, L. Wiese, M. Stirz, U. Beutling, A. Schallmey, M. Brönstrup, P. Klahn, in *Poster 34. Irseer Naturstofftage*, **2022**.

[49] T. Güngör, F. C. Önder, M. Ay, in *Recent Adv. Prodrugs* (Eds.: K. Shah, D.N. Chauhan, N.S. Chauhan, P. Mishra), Routledge, Boca Raton, **2020**, p. 26.

[50] R. Walther, J. Rautio, A. N. Zelikin, *Adv. Drug Deliv. Rev.* **2017**, *118*, 65–77.

[51] E. M. Williams, R. F. Little, A. M. Mowday, M. H. Rich, J. V. E. Chan-Hyams, J. N. Copp, J. B. Smaill, A. V. Patterson, D. F. Ackerley, *Biochem. J.* **2015**, *471*, 131–153.

[52] J. Qiao, M. Wang, M. Cui, Y. Fang, H. Li, C. Zheng, Z. Li, Y. Xu, H. Hua, D. Li, *J. Pharm. Biomed. Anal.* **2021**, *203*, 114199.

[53] M. Yuan, Y. Wu, C. Zhao, Z. Chen, L. Su, H. Yang, J. Song, *Theranostics* **2022**, *12*, 1459–1485.

[54] P. Rollin, A. Tatibouët, *Comptes Rendus Chim.* **2011**, *14*, 194–210.

https://doi.org/10.26434/chemrxiv-2024-f8x8z-v2 **ORCID:** https://orcid.org/0000-0003-4713-2345 Content not peer-reviewed by ChemRxiv. **License:** CC BY-NC-ND 4.0

[55] S. Zenno, H. Koike, M. Tanokura, K. Saigo, *J. Biochem.* **1996**, *120*, 736–744.
[56] F. J. Peterson, R. P. Mason, J. Hovsepian, J. L. Holtzman, *J. Biol. Chem.* **1979**, *254*, 4009–4014.
[57] A. Christofferson, J. Wilkie, *Biochem. Soc. Trans.* **2009**, *37*, 413–418.
[58] P. R. Race, A. L. Lovering, R. M. Green, A. Ossor, S. A. White, P. F. Searle, C. J. Wrighton, E. I. Hyde, *J. Biol. Chem.* **2005**, *280*, 13256–13264.
[59] M. W. Mullowney, N. I. Maltseva, M. Endres, Y. Kim, A. Joachimiak, T. S. Crofts, *Microbiol. Spectr.* **2022**, *10*, e00139-22.
[60] T. S. Crofts, P. Sontha, A. O. King, B. Wang, B. A. Biddy, N. Zanolli, J. Gaumnitz, G. Dantas, *Cell Chem. Biol.* **2019**, *26*, 559-570.e6.
[61] T. Nakamura, Y. Kawai, N. Kitamoto, T. Osawa, Y. Kato, *Chem. Res. Toxicol.* **2009**, *22*, 536–542.
[62] L. Petri, P. A. Szijj, Á. Kelemen, T. Imre, Á. Gömöry, M. T. W. Lee, K. Hegedűs, P. Ábrányi-Balogh, V. Chudasama, G. M. Keserű, *RSC Adv.* **2020**, *10*, 14928–14936.
[63] I. Karlsson, K. Samuelsson, D. J. Ponting, M. Törnqvist, L. L. Ilag, U. Nilsson, *Sci. Rep.* **2016**, *6*, 21203.
[64] P. R. A. Zanon, L. Lewald, S. M. Hacker, *Angew. Chem. Int. Ed.* **2020**, *59*, 2829–2836.
[65] P. R. A. Zanon, F. Yu, P. Z. Musacchio, L. Lewald, M. Zollo, K. Krauskopf, D. Mrdovic, P. Raunft, T. E. Maher, M. Cigler, C. J. Chang, K. Lang, F. D. Toste, A. I. Nesvihskii, S. M. Hacker, D. Mrdović, P. Raunft, T. E. Maher, M. Cigler, C. J. Chang, K. Lang, F. D. Toste, A. I. Nesvizhskii, S. M. Hacker, *ChemRxiv* **2021**, *1*, DOI: 10.26434/chemrxiv-2021-w7rss-v2.
[66] K. M. Backus, B. E. Correia, K. M. Lum, S. Forli, B. D. Horning, G. E. González-Páez, S. Chatterjee, B. R. Lanning, J. R. Teijaro, A. J. Olson, D. W. Wolan, B. F. Cravatt, *Nature* **2016**, *534*, 570–574.
[67] E. Weerapana, C. Wang, G. M. Simon, F. Richter, S. Khare, M. B. D. Dillon, D. A. Bachovchin, K. Mowen, D. Baker, B. F. Cravatt, *Nature* **2010**, *468*, 790–795.
[68] A. T. Kong, F. V Leprevost, D. M. Avtonomov, D. Mellacheruvu, A. I. Nesvizhskii, *Nat. Methods* **2017**, *14*, 513–520.
[69] F. Yu, G. C. Teo, A. T. Kong, S. E. Haynes, D. M. Avtonomov, D. J. Geiszler, A. I. Nesvizhskii, *Nat. Commun.* **2020**, *11*, 4065.
[70] F. Yu, S. E. Haynes, G. C. Teo, D. M. Avtonomov, D. A. Polasky, A. I. Nesvizhskii, *Mol. Cell. Proteomics* **2020**, *19*, 1575–1585.
[71] S. Grivas, E. Ronne, L. Vares, I. Kühn, A. Claesson, J. Arnarp, L. Björk, R. Gawinecki, *Acta Chem. Scand.* **1995**, *49*, 225–229.
[72] G. Clavé, H. Boutal, A. Hoang, F. Perraut, H. Volland, P. Y. Renard, A. Romieu, *Org. Biomol. Chem.* **2008**, *6*, 3065–3078.
[73] A. J. O'Neill, *Lett. Appl. Microbiol.* **2010**, *51*, 358–361.
[74] T. Rizk, E. J.-F. Bilodeau, A. M. Beauchemin, *Angew. Chem. Int. Ed.* **2009**, *48*, 8325–8327.
[75] M. J. Horsburgh, J. L. Aish, I. J. White, L. Shaw, J. K. Lithgow, S. J. Foster, *J. Bacteriol.* **2002**, *184*, 5457–5467.
[76] D. Kessner, M. Chambers, R. Burke, D. Agus, P. Mallick, *Bioinformatics* **2008**, *24*, 2534–2536.
[77] F. da Veiga Leprevost, S. E. Haynes, D. M. Avtonomov, H.-Y. Chang, A. K. Shanmugam, D. Mellacheruvu, A. T. Kong, A. I. Nesvizhskii, *Nat. Methods* **2020**, *17*, 869–870.
[78] T. Stiernagle, in *WormBook*, **2006**, pp. 51–67.
[79] J. Schindelin, I. Arganda-Carreras, E. Frise, V. Kaynig, M. Longair, T. Pietzsch, S. Preibisch, C. Rueden, S. Saalfeld, B. Schmid, J.-Y. Tinevez, D. J. White, V. Hartenstein, K. Eliceiri, P. Tomancak, A. Cardona, *Nat. Methods* **2012**, *9*, 676–682.
[80] M. Frigerio, M. Santagostino, S. Sputore, *J. Org. Chem.* **1999**, *64*, 4537–4538.
[81] Y. Nishio, R. Mifune, T. Sato, S. Ishikawa, H. Matsubara, *Tetrahedron Lett.* **2017**, *58*, 1190–1193.
[82] J. R. Guo, H. Y. Huang, Y. L. Yan, C. F. Liang, *Asian J. Org. Chem.* **2018**, *7*, 179–188.
[83] N. Dubey, P. Sharma, A. Kumar, *Synth. Commun.* **2015**, *45*, 2608–2626.
[84] M. Rauschenberg, E. C. Fritz, C. Schulz, T. Kaufmann, B. J. Ravoo, *Beilstein J. Org. Chem.* **2014**, *10*, 1354–1364.
[85] A. Brand, L. Allen, M. Altman, M. Hlava, J. Scott, *Learn. Publ.* **2015**, *28*, 151–155.

https://doi.org/10.26434/chemrxiv-2024-f8x8z-v2 **ORCID:** https://orcid.org/0000-0003-4713-2345 Content not peer-reviewed by ChemRxiv. **License:** CC BY-NC-ND 4.0

Entry for the Table of Contents

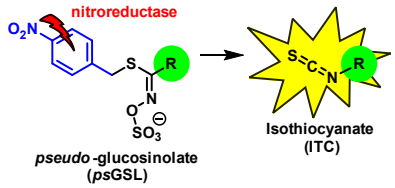

The concept of *pseudo*glucosinolates (*ps*GSLs) is introduced and synthesis and evaluation of nitroreductase-responsive *ps*GSLs is reported, representing a complementary prodrug approach to natural glucosinolates (GSLs) for the release of isothiocyanates (ITCs) for bio-responsive protein labelling demonstrated in living *C. elegans*.

Institute and/or researcher Twitter usernames: Institute and/or researcher Twitter usernames: @DocKlahn, @OMC_GU, @naturvetenskap, @goteborgsuni, @tuBraunschweig, @OCTUBS, @helmholtz_HZI, @BronstrupLab, @SieberLab, @charitySGG, @d_kagho, @StephanHacker2, @JuliaMorud

https://doi.org/10.26434/chemrxiv-2024-f8x8z-v2 **ORCID:** https://orcid.org/0000-0003-4713-2345 Content not peer-reviewed by ChemRxiv. **License:** CC BY-NC-ND 4.0